Magnetic structure of periodically meandered one-dimensional Fe nanowires

Susumu Shiraki,[1] Hideki Fujisawa,[2] Tetsuya Nakamura,[3] Takayuki Muro,[3] Masashi Nantoh,[2] and Maki Kawai[1,2]
[1]*Department of Advanced Materials Science, The University of Tokyo, 5-1-5-402 Kashiwanoha, Kashiwa, Chiba 277-8561, Japan*
[2]*RIKEN (The Institute of Physical and Chemical Research), 2-1 Hirosawa, Wako, Saitama 351-0198, Japan*
[3]*Japan Synchrotron Radiation Research Institute (JASRI)/SPring-8, 1-1-1 Kouto, Sayo, Hyogo 679-5198, Japan*
(Received 28 July 2008; published 24 September 2008)

We study the magnetic structure of perpendicularly magnetized Fe nanowires grown on Au(788) by means of x-ray magnetic circular dichroism. The average size of ferromagnetic domains in the nanowires exponentially decreases with temperature, leading to a steeper decay in magnetization compared to nanoislands of Fe. The temperature dependence of magnetization and domain structures can be well described in terms of local atomic geometry, the number of atomic chains in nanowires, exchange coupling between adjacent spins, and magnetic anisotropy. The nonlinear coverage dependence of the activation energy for the creation of magnetic domains can be explained by overall shape of nanowires, which also implies that the magnetic switching processes are strongly shape dependent at the nanoscale.

DOI: 10.1103/PhysRevB.78.115428 PACS number(s): 75.20.−g, 75.60.Jk, 75.75.+a

I. INTRODUCTION

One-dimensional (1D) surface structures have been attracting a great deal of attention because of characteristic physical phenomena observable in 1D, such as Peierls instability, quantization of conductance, and spin-charge separation (Tomonaga-Luttinger liquid). Besides these interests in the fundamental physics in low dimensions, 1D nanostructures are promising candidates for future data storage devices. In particular, the ultimate density limit of magnetic recording may be achieved for out-of-plane magnetic nanotapes because the demagnetizing field energy is reduced for antiparallel domain configurations, thereby, stabilizing recorded magnetic states against thermal agitation. The self-organized growth of 1D nanostructures on vicinal surfaces has been extensively studied from this point of view.[1–5] Controlling the magnetic properties of such systems is a key technology for the future progress in nanoelectronics and spintronics.

Through the theoretical and experimental works carried out over the past few decades there is widely accepted consensus on the magnetism of nanostructures.[6,7] The transition temperatures from ferromagnetic to paramagnetic phases are reduced with reduced size of the systems.[2,8] The magnetic moments and magnetic anisotropy are considerably enhanced compared to equivalent bulk systems,[4,5,9–12] where perimeter atoms of the nanostructures play an important role in magnetism.[12–14] However, there have been few studies of temperature and shape dependence of magnetic domain structure in 1D nanowires, which is quite different from that of two-dimensional (2D) nanoislands. In general, when the size of islands is reduced less than about 100 nm in diameter, the islands show single-domain structures where the magnetic moments of all atoms are ferromagnetically aligned. In 1D nanowires, by contrast, the single-domain structure (long-range ferromagnetic order) breaks down by thermal fluctuations, and the number of magnetic domains increases as the temperature increases. Most importantly, 1D nanowires show various types of domain structures depending on the atomic geometry, exchange coupling between adjacent spins, surface and interface anisotropy, and overall shape of nanowires.

It is well known that Au(111) surface exhibits a unique surface reconstruction[15,16] and 2D spin-polarized surface state induced by the Rashba spin-orbital coupling.[17] Dosing a very small amount of transition metals on the Au(111) and its vicinal surfaces provides a variety of nanostructures[10–13,18–20] and modifies the electronic properties of the surfaces.[21–23] The growth of Fe on a vicinal Au(111) surface is impressive as illustrated in Fig. 1. Our previous scanning tunneling microscopy (STM) observations[23] revealed that dosed Fe atoms are trapped at step edges and form 1D monatomic chains in the initial stage of the growth. As the coverage is increased, 1D Fe nanowires with a height of a single atomic layer grow in a step-flow growth mode. The shape of the nanowires and the periodicity of the nanowire arrays are homogeneous. However, due to the faster growth in fcc regions than in hcp regions, the width of the nanowires is not homogeneous but slightly fluctuates along the nanowires above ~0.3 ML. Subsequently, the Fe stripes partially reach the adjacent ones in the fcc regions, and 2D networks are built up around 0.6 ML. This feature could offer good advantages in the measurement of shape-dependent magnetization of the nanowires.

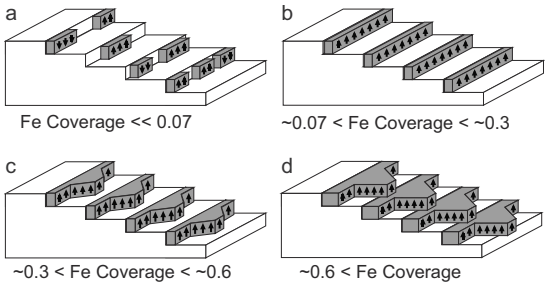

FIG. 1. Schematics of the growth manner of Fe on a Au(788) surface. (a) 1D fragments of Fe below 0.07 ML. (b) Complete formation of 1D monatomic Fe chains at 0.07 ML, and smooth 1D nanowires between 0.07 and 0.3 ML. (c) Periodically meandered quasi-1D nanowires of Fe between 0.3 and 0.6 ML. (d) 2D networks of Fe above 0.6 ML.

In this study, we fabricate precisely controlled 1D Fe nanowires on vicinal Au(111) and investigate their magnetism using x-ray absorption spectroscopy (XAS) combined with magnetic circular dichroism (XMCD). The XAS/XMCD is a powerful and suitable technique for studying magnetic properties of such nanostructures at surfaces since the sensitivity is three orders of magnitude higher compared to a conventional superconducting quantum interference device (SQUID) technique. In order to examine the magnetic domain structures of perpendicularly magnetized Fe nanowires, we perform *in situ* measurements of the temperature dependence of magnetization with XMCD. We analyze magnetization curves using a macrospin model describing superparamagnetic nanowires and discuss the magnetization reversal behavior of the 1D nanowires in terms of local atomic coordination and overall shape of nanowires.

II. EXPERIMENT

We employed Au(111) and Au(788) crystals as substrates.[24] The samples were prepared by extensive sputtering-annealing cycles until low-energy electron-diffraction (LEED) patterns displayed the characteristic spot splitting.[24] After cooling the sample to RT, Fe was dosed with an electron-beam evaporator, and Fe nanowires were fabricated below the coverage of 0.6 ML Fe by the step-flow growth on Au(788). Since each terrace consists of 16 atomic rows on Au(788), the coverage of 0.07 ML corresponds to the formation of monatomic Fe chains on this surface. The flux of Fe during evaporation was measured with a quartz-crystal film-thickness monitor. A typical deposition rate was about 0.05 ML/min. The coverage of Fe on the Au surface was determined by the flux and evaporation time and checked by absorption intensity in XAS. The *in situ* synchrotron radiation (SR) experiments were subsequently carried out after the sample preparation at the soft x-ray undulator beamline BL25SU at SPring-8.[25] In the beamline, circularly polarized soft x-ray from a twin helical undulator was monochromatized and focused on the sample through pinholes of a permanent magnet circuit. X-ray absorption spectra were measured by the total electron yield method in which the sample current is directly measured while scanning the photon energy. The magnetic field up to 1.9 T was applied in the direction perpendicular to the surface. The SR beam was incident on the samples at 10° away from the surface-normal direction. Since MCD signals depend on the scalar product of the SR beam and sample magnetization, the MCD intensities correspond to the perpendicular magnetization of Fe on the Au surfaces.

III. RESULTS AND DISCUSSION

Figures 2(a) and 2(b) show XAS and XMCD spectra for 1D double atomic chains of Fe (0.14 ML), respectively. Fe $L_{2,3}$ absorption edges in XAS are related to excitations from $2p$ core level into unoccupied $3d$ valence states. The MCD spectrum is obtained from the difference between the XAS spectra recorded for the photon helicity parallel (μ_+) and antiparallel (μ_-) to the $3d$ majority-spin direction under the external field of $H=1.9$ T. The MCD intensity is normalized with the edge jump at the L_3 peak in the XAS spectrum, and thus the peak intensity in MCD corresponds to the magnetic moments per Fe atom. It is well known that the local-orbital m_L and spin m_s magnetic moments can be deduced using the sum rules.[26–28] Although the number of holes in the $3d$ band is unknown in the present case of the Fe nanowire, we can obtain the orbital to effective spin moment ratio by canceling it,

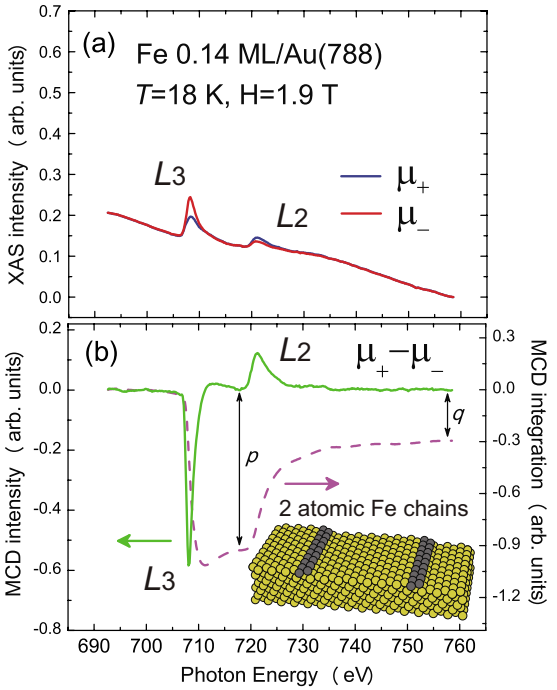

FIG. 2. (Color online) (a) XAS and (b) MCD spectra for 1D double atomic chains of Fe on Au(788). Fe $L_{2,3}$ absorption edges in XAS are related to excitations from $2p$ core level into unoccupied $3d$ valence states. The MCD spectrum is obtained from the difference between the XAS spectra recorded for the photon helicity parallel (μ_+) and antiparallel (μ_-) to the $3d$ majority-spin direction under the external field of $H=1.9$ T. The MCD signal is normalized with the edge jumps at the L_3 in the XAS spectrum. The dashed line in (b) is the MCD integration calculated from the MCD spectrum, and p and q are integrals needed in the sum-rule analysis.

$$m_L/m_s^{\mathrm{eff}} = 2q/(9p - 6q), \tag{1}$$

where p and q are the integrals over L_3 and (L_3+L_2) peaks of the XMCD spectrum, respectively [Fig. 2(b)]. From the XMCD spectrum, we obtained $m_L/m_s^{\mathrm{eff}}=0.15\pm0.02$, which is three times as large as 0.05 obtained for 2D Fe monolayer, and is almost half of 0.26 obtained for monatomic Fe chains.[29] As mentioned in Sec. I, such an enhancement of the orbital magnetic moment for reduced coverages is a general phenomenon, and a similar result was also observed in the case of 1D Co nanowires grown on a Pt(997) surface.[5]

Figure 3(a) displays the temperature dependence of magnetization at different coverages of Fe on Au(788). We found that as the coverage is reduced, the 1D nanowires show a faster decay with T. Furthermore, a remarkable trend is observed in a comparison between the nanowires and nanois-

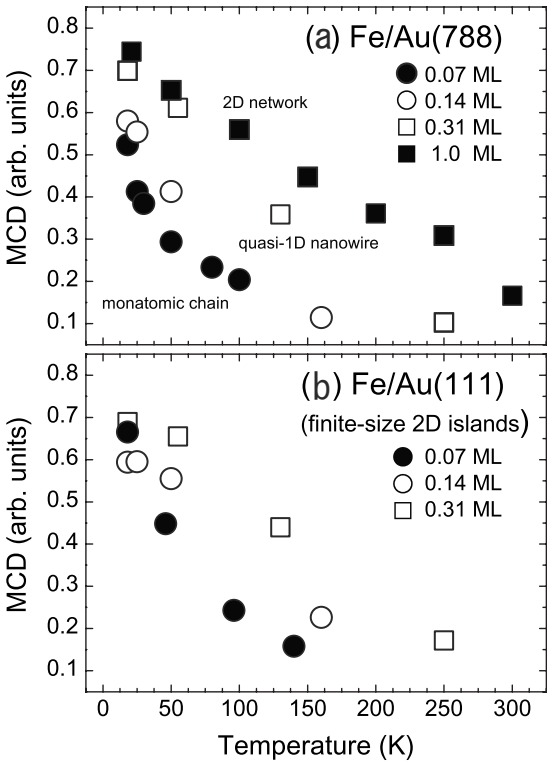

FIG. 3. Temperature dependence of magnetization per Fe atom (a) for 1D nanowires on Au(788) and (b) for 2D nanoislands on Au(111). MCD spectra were obtained at each temperature and peak intensities at the Fe L_3 absorption edge were plotted as a function of temperature T.

lands grown on Au(111),[11,18,30] as shown in Fig. 3(b). The magnetization of the 1D nanowires decays faster with T and is always less than that of the nanoislands of the same coverage. These results are intuitively understandable if we consider low phase-transition temperatures and intense thermal fluctuation effects in lower dimensions. However, details of magnetic domain structures in the nanowires and their temperature dependence are more complicated compared with those of the nanoislands. In the case of 1D ferromagnetic nanowires, even if all the moments are initially aligned, spin flip takes place, and then the nanowires are inevitably broken up into shorter domains at finite temperatures, which is in contrast to the single magnetic domains of the nanoislands. When we describe the magnetism in nanowires, we must consider the formation of the magnetic domains and the motion of their boundaries in 1D. To this end, we examine the temperature dependence of magnetization curves in the following.

Figure 4 shows magnetization curves for [Fig. 4(a)] monatomic chains (0.07 ML), [Fig. 4(b)] double atomic chains (0.14 ML), [Fig. 4(c)] quasi-1D nanowires (0.31 ML), and [Fig. 4(d)] 2D monolayer (1.0 ML) of Fe on Au(788), respectively. We can clearly see the phase transitions from blocking to superparamagnetic behavior with an easy axis perpendicular to the surface although the transition temperature is different for each coverage. At the lowest temperatures, the magnetization curves show hysteresis loops where each domain is blocked in a fixed magnetization state (up or down) as a result of freezing of thermal fluctuation. However, the curves are not simple squarelike hysteresis loops,

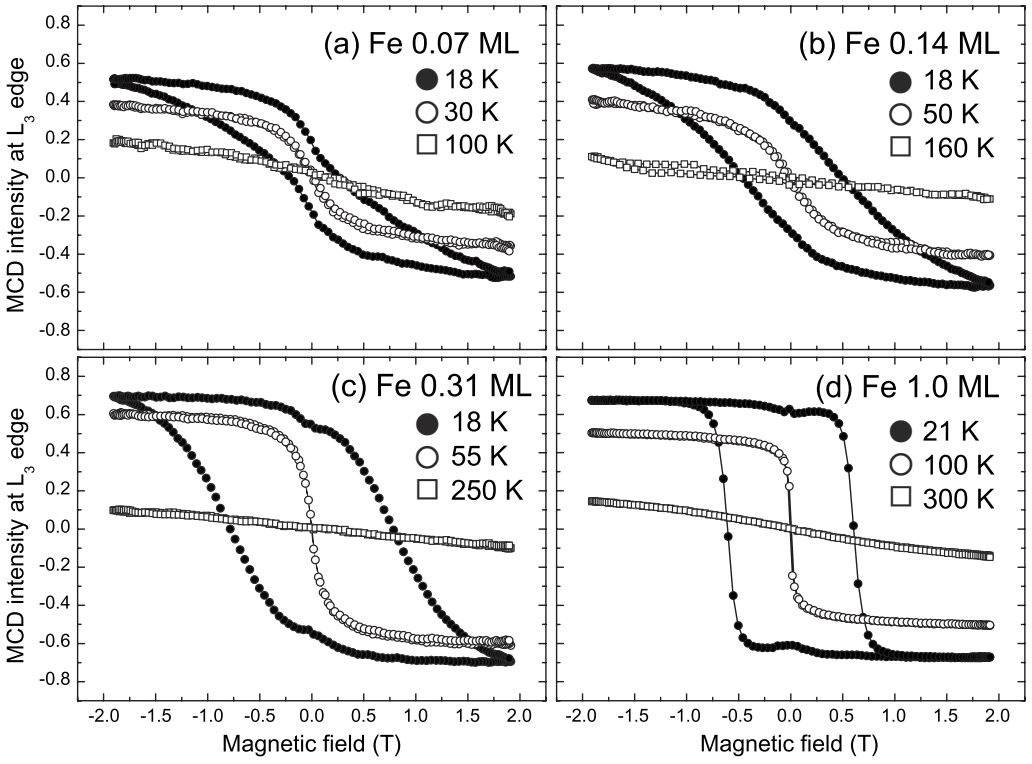

FIG. 4. Magnetization curves of Fe nanostructures grown on Au(788). (a) 1D monatomic chains (0.07 ML). (b) 1D double atomic chains (0.14 ML). (c) Quasi-1D nanowires (0.31 ML). (d) 2D monolayer (1.0 ML). MCD intensities were recorded with the photon energy at the Fe L_3 absorption edge of 708 eV, which corresponds to the magnetization of the Fe nanostructures per atom.

and remanence at zero field is much smaller than the saturation magnetization. This implies that thermal fluctuation seems to be still not negligible in the 1D systems. As the temperature increases, the coercive field disappears at T_B, which is called blocking temperature. This temperature is related to the magnetic anisotropy energy for a magnetic domain, which works as an energy barrier for flips of the macrospins. Above T_B, the magnetization spontaneously reverses because of thermal agitation, and the typical superparamagnetic reversible S-shaped curves are observed. In general, the reversal behavior can be described within a simple macrospin model as discussed below.

Before analyzing the magnetization curves in terms of magnetic moments and anisotropy energies, we explain a macrospin model describing the superparamagnetism of an ensemble of non-interacting magnetic 1D fragments in nanowires. Gambardella *et al.*[4] applied the macrospin model to 1D monatomic Co chains on a Pt(997) surface. We also assume that each Fe atom has the same magnetic moment m; thus the moment of each domain containing N atoms is given by $M=Nm$ in average. Analogously, the magnetic anisotropy of each domain is given by $E_a=\mathrm{Ne}_a$, where e_a is the anisotropy per Fe atom. Hence, the magnetization curves can be described by modified Langevin function,[4]

$$M = M_{\mathrm{sat}} \frac{\int_0^{\pi} d\theta \sin\theta \cos\theta e^{N(mB\cos\theta + e_a \cos^2\theta)/k_B T}}{\int_0^{\pi} d\theta \sin\theta e^{N(mB\cos\theta + e_a \cos^2\theta)/k_B T}}. \quad (2)$$

By fitting the Langevin function to the magnetization curves obtained above T_B, we derived average numbers (N) of Fe atoms per domain and plot them as functions of temperature in Fig. 5(a).[31] As we expected, the average size of magnetic domains rapidly decreases with increasing temperature at each coverage. This is probably a major reason why the magnetization of 1D nanowires exhibits a steeper decay with temperature compared to nanoislands, as shown in Fig. 3.

Next, we explain a simple 1D spin model describing the magnetic domains in nanowires, as shown in Fig. 5(b). Now we first consider the monatomic chains ($W=1$). Since the nearest-neighbor interaction is dominant, the activation energy for the creation of a domain corresponds to $4J$, where J is the coupling energy between adjacent spins ($J>0$ for ferromagnetic coupling). In this case, the probability of spin flips increases with temperature and is given by $p=A\exp(-4J/k_BT)$ as a function of temperature T. Hence, the temperature dependence of N can be described as

$$N(T) = N_0 \exp(4J/k_B T), \quad (3)$$

and $J=0.55$ meV is obtained for monatomic Fe chains (see Ref. 29 for details). Analogously, the 1D nanowires can be considered using the model for W parallel atomic chains. Since a domain boundary has n ($=2W-1$) pairs of antiparallel spins, the activation energy of $2nJ$ is necessary for the creation of a domain boundary and thus $4nJ$ for the creation of a domain. Consequently, the number of Fe atoms per domain is given by

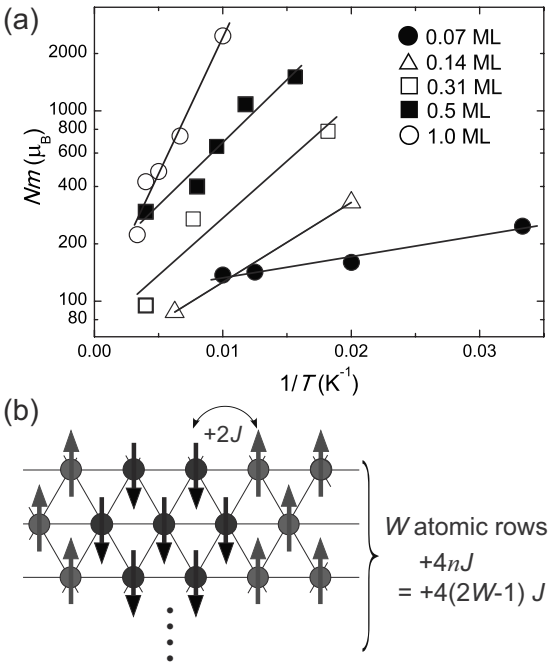

FIG. 5. (a) Temperature dependence of the average number of Fe atoms per magnetic domain obtained by fitting the Langevin function to the magnetization curves of Fig. 4. (b) Schematics of the creation of a magnetic domain in 1D nanowires for W parallel atomic chains. The black and gray atoms are magnetized into and out of the surface, respectively.

$$N(T) = N_0 \exp[4(2W-1)J/k_B T] \quad (4)$$

for W atomic rows. As expected from the equation, the slope of the Arrhenius plots of Nm in Fig. 5(a) increases with W, and we obtain $4nJ=8.3$, 12, 13, and 29 meV for 0.14, 0.31, 0.5, and 1.0 ML, respectively. Assuming constant J in the submonolayer range, we further obtain $n=3.7$, 5.5, and 6 for 0.14, 0.31, and 0.5 ML using the J value of 0.55 meV for the monatomic chains.

In Fig. 6(a), $4nJ$ is plotted as a function of Fe coverage. It is worth noting that Fig. 6(a) shows a nonlinear dependence of $4nJ$ contrary to what one might expect. If the growth of the nanowires ideally proceeds in the step-flow growth mode, $4nJ$ would be proportional to the coverage. Particularly in the case of 0.31 and 0.5 ML, the obtained values of $4nJ$ are much smaller than the expected values obtained from the relation $n=2W-1$: $4nJ=18.7$ meV for 0.31 ML and 33 meV for 0.5 ML. A plausible explanation for this deviation is the periodically meandered shapes of the quasi-1D nanowires as illustrated in Fig. 6(b). Since structural constrictions often serve as nucleation, annihilation, and pinning centers for domain boundaries, $4nJ$ becomes smaller than the values expected from the average width of the nanowires. Hence, we can derive the number W_b of atomic chain at the constrictions from the experimental data and obtained $W_b=3.2$ for 0.31 ML and $W_b=3.5$ for 0.5 ML. These values are in good agreement with our previous STM observations,[23] which estimated the width of the narrower regions in meandered structures to be three to four atomic rows. Hence we can conclude that the magnetic domain structures in 1D Fe nano-

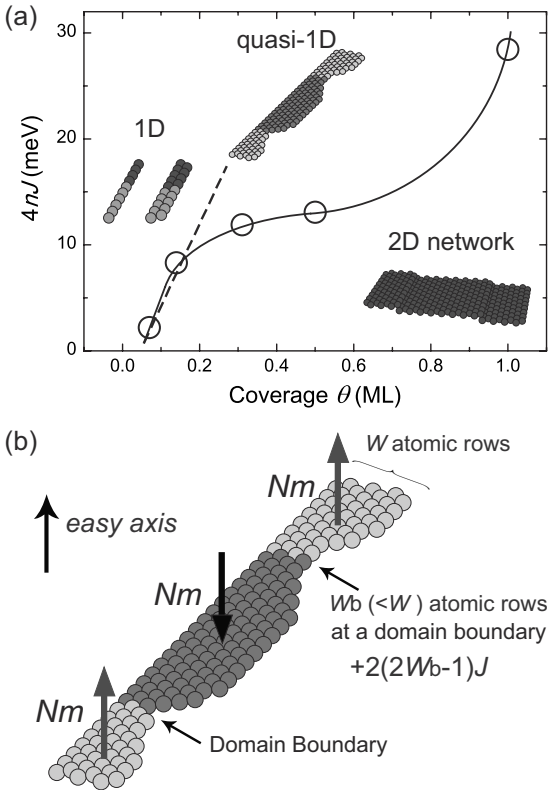

FIG. 6. (a) The activation energy $4nJ$ for the creation of a magnetic domain as a function of coverage. The solid line is a guide for eyes. The dashed line corresponds to the relations of $4nJ=4(2W-1)J$ in Fig. 5(b). (b) Magnetic domain structure in periodically meandered 1D nanowires of Fe. The black and gray atoms are magnetized into and out of the surface, respectively. Since domain boundaries appear at the narrowed regions of the nanowires, the number W_b of atomic chain at the boundaries is smaller than the average width of the nanowires.

wires on Au(788) strongly depend on the overall shape of the nanowires.

Finally, we focus on magnetization reversal in 1D monatomic chains, quasi-1D stripes, and 2D networks of Fe. Our results provide a clear insight into the shape-dependent magnetization processes in the 1D nanowires. In the case of monatomic and double atomic chains, magnetization processes are based on the single spin flips, and domain boundaries can move site by site. In the case of the quasi-1D nanowires by contrast, the domain boundaries appear and are pinned at the narrower regions in the meandered 1D structures, which give the smallest domain boundary energy. Therefore, magnetization reversal occurs as the macrospins inside the domains flip to the opposite direction. Finally, the magnetization processes drastically change when the 2D networks of Fe are built up around the coverage of 0.6 ML. Superparamagnetic fluctuation must be strongly suppressed due to large $4nJ$ leading to a remanence-to-saturation ratio of nearly 1 [Fig. 4(d)] and the coherent rotation of entire magnetization under the action of the external field.

IV. CONCLUSIONS

We performed an XMCD study of the perpendicularly magnetized 1D Fe nanowires grown on Au(788). The XMCD spectrum shows that the orbital magnetic moments are enhanced in 1D nanowires, but the large magnetic moments are rapidly suppressed with elevated temperature due to the intensive fluctuation in lower dimensions. From the temperature dependence of XMCD-magnetization loops, we found magnetic phase transitions from ferromagnetic to superparamagnetic state in 1D Fe nanowires. The simple analysis using the macrospin model revealed that the average domain size rapidly decreases as the temperature increases, following the Arrhenius law ruled by exchange energy and the number of antiparallel spin pairs at the boundaries. Our findings attest to the importance of local atomic geometry, exchange coupling, and magnetic anisotropy for the understanding of the magnetism in 1D nanowires. Particularly, the size and overall shape of nanowires have decisive influence on domain patterns and thus on magnetic properties. Periodically meandered nanowires or nanotapes might be a suitable shape, which will allow the ultimate high density of magnetic storage media. Further work of these systems is needed to show a direct observation of magnetic domain structures and the magnetization processes using microscopic techniques such as spin-polarized STM.

ACKNOWLEDGMENTS

We thank S. Itoh and M. Furukawa for their help during the experiments. The SR experiments were performed at SPring-8 with the approval of JASRI (Proposal No. 2004B0523-NSc-np-Na/0774-NSc-np) as Nanotechnology Support Project of the Ministry of Education, Culture, Sports, Science and Technology (MEXT). This research work was financially supported by Grant-in-Aid for Young Scientists (A) (No. 20681012), Grant-in-Aid for Scientific Research on Priority Areas, "Electron transport through a linked molecule in nanoscale" (No. 17069005), and Global COE Program "the Physical Sciences Frontier," MEXT.

[1] H. J. Elmers, J. Hauschild, H. Höche, U. Gradmann, H. Bethge, D. Heuer, and U. Köhler, Phys. Rev. Lett. **73**, 898 (1994).
[2] J. Shen, R. Skomski, M. Klaua, H. Jenniches, S. S. Manoharan, and J. Kirschner, Phys. Rev. B **56**, 2340 (1997).
[3] O. Pietzsch, A. Kubetzka, M. Bode, and R. Wiesendanger, Science **292**, 2053 (2001).
[4] P. Gambardella, A. Dallmeyer, K. Maiti, M. C. Malagoli, W. Eberhardt, K. Kern, and C. Carbone, Nature (London) **416**, 301 (2002).
[5] P. Gambardella, A. Dallmeyer, K. Maiti, M. C. Malagoli, S. Rusponi, P. Ohresser, W. Eberhardt, C. Carbone, and K. Kern, Phys. Rev. Lett. **93**, 077203 (2004).
[6] F. J. Himpsel, J. E. Ortega, G. J. Mankey, and R. F. Willis, Adv. Phys. **47**, 511 (1998).

[7] O. Fruchart and A. Thiaville, C. R. Phys. **6**, 921 (2005).
[8] D. Li, B. R. Cuenya, J. Pearson, S. D. Bader, and W. Keune, Phys. Rev. B **64**, 144410 (2001).
[9] P. Gambardella, S. Rusponi, M. Veronese, S. S. Dhesi, C. Grazioli, A. Dallmeyer, I. Cabria, R. Zeller, P. H. Dederichs, K. Kern, C. Carbone, and H. Brune, Science **300**, 1130 (2003).
[10] T. Koide, H. Miyauchi, J. Okamoto, T. Shidara, A. Fujimori, H. Fukutani, K. Amemiya, H. Takeshita, S. Yuasa, T. Katayama, and Y. Suzuki, Phys. Rev. Lett. **87**, 257201 (2001).
[11] P. Ohresser, N. B. Brookes, S. Padovani, F. Scheurer, and H. Bulou, Phys. Rev. B **64**, 104429 (2001).
[12] H. A. Dürr, S. S. Dhesi, E. Dudzik, D. Knabben, G. van der Laan, J. B. Goedkoop, and F. U. Hillebrecht, Phys. Rev. B **59**, R701 (1999).
[13] N. Weiss, T. Cren, M. Epple, S. Rusponi, G. Baudot, S. Rohart, A. Tejeda, V. Repain, S. Rousset, P. Ohresser, F. Scheurer, P. Bencok, and H. Brune, Phys. Rev. Lett. **95**, 157204 (2005).
[14] S. Rusponi, T. Cren, N. Weiss, M. Epple, P. Buluschek, L. Claude, and H. Brune, Nat. Mater. **2**, 546 (2003).
[15] Ch. Wöll, S. Chiang, R. J. Wilson, and P. H. Lippel, Phys. Rev. B **39**, 7988 (1989).
[16] J. V. Barth, H. Brune, G. Ertl, and R. J. Behm, Phys. Rev. B **42**, 9307 (1990).
[17] S. LaShell, B. A. McDougall, and E. Jensen, Phys. Rev. Lett. **77**, 3419 (1996).
[18] B. Voigtlander, G. Meyer, and N. M. Amer, Surf. Sci. **255**, L529 (1991).
[19] S. Rohart, Y. Girard, Y. Nahas, V. Repain, G. Rodary, A. Tejeda, and S. Rousset, Surf. Sci. **602**, 28 (2008).
[20] S. Shiraki, H. Fujisawa, M. Nantoh, and M. Kawai, Surf. Sci. **552**, 243 (2004).
[21] C. Didiot, S. Pons, B. Kierren, Y. Fagot-Revurat, and D. Malterre, Nat. Nanotechnol. **2**, 617 (2007).
[22] S. Shiraki, H. Fujisawa, M. Nantoh, and M. Kawai, Phys. Rev. Lett. **92**, 096102 (2004).
[23] S. Shiraki, H. Fujisawa, M. Nantoh, and M. Kawai, J. Phys. Soc. Jpn. **74**, 2033 (2005).
[24] A. Mugarza, A. Mascaraque, V. Pérez-Dieste, V. Repain, S. Rousset, F. J. García de Abajo, and J. E. Ortega, Phys. Rev. Lett. **87**, 107601 (2001).
[25] T. Nakamura, T. Muro, F. Z. Guo, T. Matsushita, T. Wakita, T. Hirono, Y. Takeuchi, and K. Kobayashi, J. Electron Spectrosc. Relat. Phenom. **144-147**, 1035 (2005).
[26] B. T. Thole, P. Carra, F. Sette, and G. van der Laan, Phys. Rev. Lett. **68**, 1943 (1992).
[27] P. Carra, B. T. Thole, M. Altarelli, and X. Wang, Phys. Rev. Lett. **70**, 694 (1993).
[28] C. T. Chen, Y. U. Idzerda, H.-J. Lin, N. V. Smith, G. Meigs, E. Chaban, G. H. Ho, E. Pellegrin, and F. Sette, Phys. Rev. Lett. **75**, 152 (1995).
[29] H. Fujisawa, S. Shiraki, M. Furukawa, S. Ito, T. Nakamura, T. Muro, M. Nantoh, and M. Kawai, Phys. Rev. B **75**, 245423 (2007).
[30] Dosed Fe atoms aggregate and form Fe nanoislands at elbows of the herringbone zigzag reconstruction on the Au(111) surface, leading to a periodic array of the Fe nanoislands.
[31] Since m is unknown in the present case of the Fe nanowire, we plotted not N but Nm as a function of temperature T in Fig. 5(a) for further data analysis.